Electrical Transport and Confocal Raman Studies of Electrochemically Modified Individual Carbon Nanotubes**

By *Kannan Balasubramanian*, *Marcel Friedrich*, *Chaoyang Jiang*, *Yuwei Fan*, *Alf Mews*, *Marko Burghard*,* and *Klaus Kern*

Single-walled carbon nanotubes (SWCNTs), due to their excellent structural and electronic properties,[1] have emerged as an attractive material for various applications including molecular electronics[2,3] and field emission devices.[4] A variety of devices have been realized with SWCNTs, such as single electron transistors (SETs) operating at very low temperatures,[5] field-effect transistors (FETs),[6] chemical sensors,[7] and logic circuits.[8] Besides the use of pristine SWCNTs, it has been shown that SWCNTs can be chemically modified,[9–11] a process which, for example, allowed the fabrication of SETs[12] and memory devices[13] operating at room temperature. Electrochemistry is a well-suited tool for controlled modification of SWCNTs.[14] This approach has been followed using both reductive and oxidative coupling schemes, resulting in thin layers of molecules around the SWCNTs.[15] However, little is known about the nature of chemical coupling between the grafted layers and the carbon framework of an individual nanotube, and also about the effect of chemical modification on its electronic properties. Towards this objective, we report in this communication the detailed investigation of individual electrochemically modified SWCNTs. The characterization methods include electrical transport measurements and confocal Raman spectroscopy, both of which can address selected single SWCNTs or bundles. While transport measurements give information about the electronic properties of an individual SWCNT, confocal Raman spectroscopy on individual nanotubes[16] can detect changes of the vibrational properties and hence the disturbances in the lattice structure of an isolated nanotube. These studies were performed separately on metallic and semiconducting SWCNTs, in both cases comparing the effect of the oxidative and reductive coupling schemes.

The electrochemical modification (ECM) of individual SWCNTs was performed with 4-aminobenzylamine (**A**) using the oxidative scheme and with 4-nitrobenzene diazonium tetrafluoroborate (**B**) employing the reductive scheme. The transport measurements were carried out on the same SWCNTs before and after ECM. Before ECM, the gate dependence of the 2-probe resistance was used to identify a given individual SWCNT as metallic or semiconducting. At room temperature, the unmodified metallic SWCNTs showed a 2-probe resistance in the range 10–25 kΩ, while the resistance of the semiconducting nanotubes was found to vary between 200 kΩ and 100 MΩ among different samples. As control experiments, ECM was performed on selected SWCNTs in the pure electrolyte solution in the absence of **A** or **B**. In both cases, neither an increase in height nor a change in the resistance could be detected after modification.

Figure 1 summarizes a typical observation made on metallic SWCNTs after oxidative ECM. The SWCNTs were investigated by atomic force microscopy (AFM) before and after ECM to determine the thickness of the grafted layers. The AFM image in Figure 1a shows an individual metallic nanotube contacted underneath four separately addressable electrodes. After modification of the nanotube with **A** by applying a positive potential (+0.75 V vs. Pt for 120 s) on electrode number 3, its height is homogeneously increased as can be seen from the AFM image in Figure 1b. The specific conditions used in the electrochemical modification resulted in a thickness increase of ~3 nm, which is determined from the difference in the height profiles (Fig. 1c) taken along the lines marked in the AFM images between electrodes 3 and 4, before and after ECM. The current–voltage (*I*–*V*) characteristics measured between electrodes 3 and 4 are compared before and after ECM in Figure 1d. It is apparent that even though the nanotube is clearly coated with a layer of **A**, the initial resistance of 17 kΩ is essentially preserved after modification. In contrast, resistance increases by up to three orders of magnitude were observed in most cases after reductive coupling of **B** (–1.3 V vs. Pt for 120 s) to metallic SWCNTs.

Oxidative and reductive ECM were also performed on individual semiconducting SWCNTs. In contrast to the metallic nanotubes, the oxidative coupling of **A** to semiconducting nanotubes was found to increase the resistance. For example, Figure 2a shows the *I*–*V* curves before and after the deposition of a 4 nm thick layer, which leads to a resistance change of the nanotubes by one order of magnitude. On the other hand, after reductive diazonium coupling onto semiconducting SWCNTs (Fig. 2b), a greater increase in resistance of around two to three orders of magnitude was observed for most samples, similar to the case of metallic nanotubes.

The electrical transport studies have been complemented by confocal Raman spectroscopy on the same individual SWCNTs before and after ECM. The main features in the Raman spectrum of SWCNTs are the radial breathing mode (RBM) in the frequency range up to 250 cm^{-1} which is sensitive to the nanotube diameter, the so called G-line around 1600 cm^{-1} originating from the tangential vibrations of the carbon atoms, and the D-line at about 1300 cm^{-1}.[17] The intensity of the D-line is related to the amount of sp^3 defects within the nanotubes, which lower the crystal symmetry of the sp^2 material.[18] Therefore, we concentrate on the changes in the D-line intensities brought about by ECM. The absolute intensity of the D-line in the Raman spectra cannot be used di-

[*] Dr. M. Burghard, K. Balasubramanian, Dr. Y. Fan, Prof. K. Kern
Max-Planck-Institut für Festkörperforschung
Heisenbergstrasse 1, D-70569 Stuttgart (Germany)
E-mail: m.burghard@fkf.mpg.de
M. Friedrich, Dr. C. Jiang, Dr. A. Mews
Institut für Physikalische Chemie, Universität Mainz
D-55099 Mainz (Germany)

[**] This work was supported by the BMBF (contract No. 03C0302B9), and the DFG (Schwerpunktprogramm organische Feldeffekt-Transistoren). We are grateful to Dr. R. Sordan for his help with sample preparation.

 DOI: 10.1002/adma.200305129

ADVANCED MATERIALS

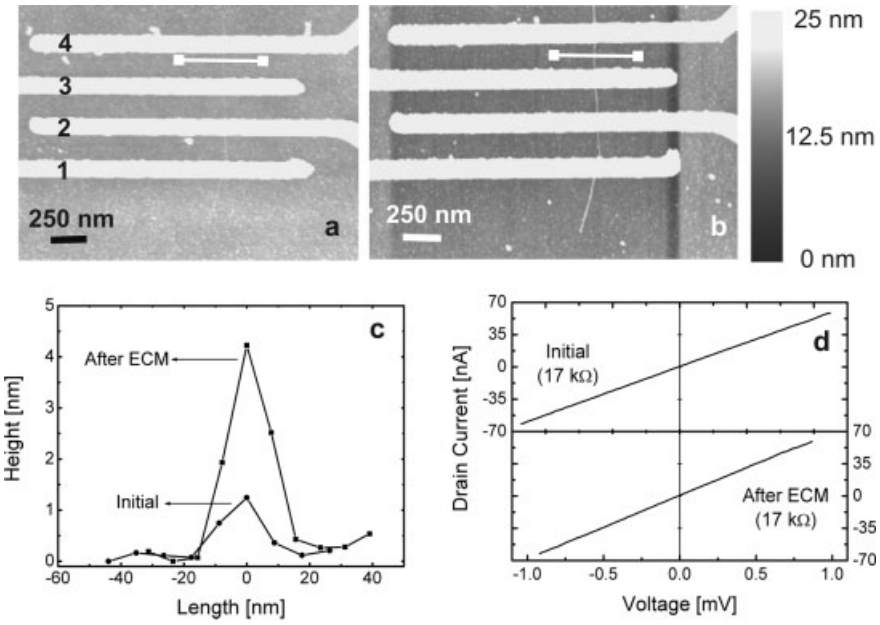

Fig. 1. Oxidative ECM of an individual metallic SWCNT with **A**: a) AFM image of the SWCNT lying below the electrodes numbered 1 to 4 before ECM. b) AFM image of the same region after ECM on electrode 3 with **A** (+0.75 V vs. Pt, 120 s). c) Comparison of the height of the SWCNT before and after ECM along the line marked in the AFM images. d) Current–voltage (*I*–*V*) curves of the SWCNT before and after ECM between electrodes 3 and 4.

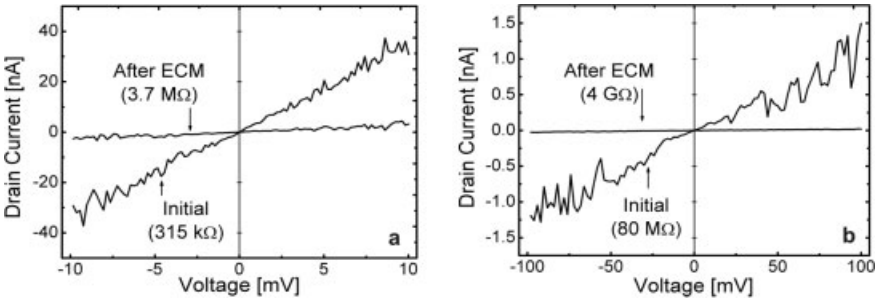

Fig. 2. ECM on semiconducting SWCNTs: a) *I*–*V* curve of a semiconducting SWCNT before and after oxidative ECM with 4-aminobenzylamine. b) *I*–*V* curve of another semiconducting SWCNT before and after reductive ECM with 4-nitrobenzene diazonium salt.

rectly for comparison, since the amount of light falling on the SWCNT can be different at different instances, due to the finite size of the diffraction-limited spot. Hence, we focus here on the effect of ECM on the relative intensity of the D-line with respect to the G-line to gain a qualitative measure of the structural disturbance of the SWCNTs. In order to distinguish metallic from semiconducting nanotubes, we made use of the selective resonant enhancement of the Raman signal. For the samples investigated in this work a wavelength of 514.5 nm was used to excite mainly the semiconducting SWCNTs while the metallic SWCNTs were resonantly excited at a wavelength of 647.1 nm.[19] As an illustration of the applied method, Figures 3a and b show the AFM and confocal G-line Raman images of the same SWCNTs (-bundles) before ECM. Since the Raman image was obtained by excitation with 647.1 nm, the visible objects correspond to either individual metallic nanotubes or bundles that contain at least one metallic nanotube.

After ECM and topological characterization by AFM, the confocal Raman imaging was repeated and the spectra were taken at the same locations as before. The Raman spectra of the metallic nanotube marked "*x*" in Figures 3a,b are compared before and after modification in Figure 3c. It is clear that there is only a negligible change in the relative intensity of the G- and D-lines. Moreover, within the accuracy of the

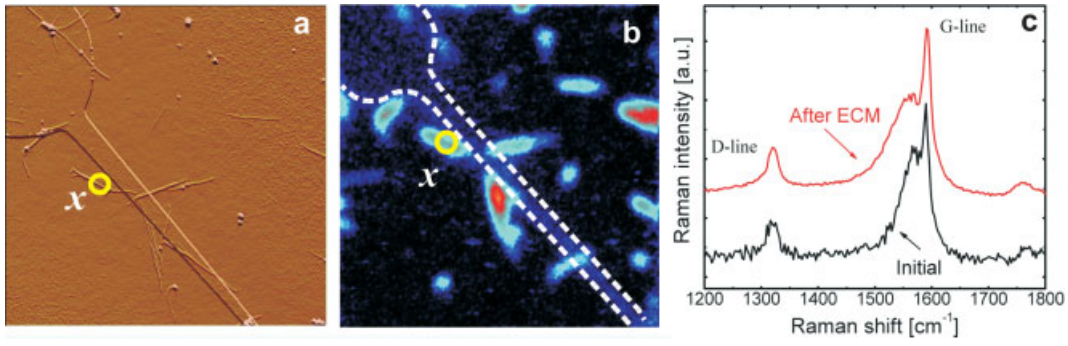

Fig. 3. Characterization of SWCNTs modified by oxidative ECM through confocal Raman spectroscopy: a) AFM image of the sample showing an electrode and the SWCNTs (8 μm × 8 μm); b) a confocal G-line Raman image (10 μm × 10 μm) of the same sample taken with an excitation wavelength of 647.1 nm. The electrode structure is drawn in white, the background appears dark blue and the SWCNTs appear as light blue to red regions; c) Raman spectra showing the D-line and G-line of the SWCNT marked × before and after ECM. The changes in the intensity and shift in the frequency of these two features are negligible in this case.

experimental setup, no shift in the Raman frequencies was observable. The same series of measurements have also been carried out on semiconducting SWCNTs ($\lambda_{exc} = 514.5$ nm). Also in this case neither a change in the D- to G-line intensity ratio, nor a shift in the frequency could be observed.

Different behavior was observed in the Raman spectra for the reductive diazonium coupling to the nanotubes. Figures 4a,b show typical spectra before and after reductive ECM observed on metallic ($\lambda_{exc} = 647.1$ nm) and semiconducting SWCNTs ($\lambda_{exc} = 514.5$ nm) respectively. It is clear that the relative intensity of the D-line is strongly increased upon chemical modification in both cases.

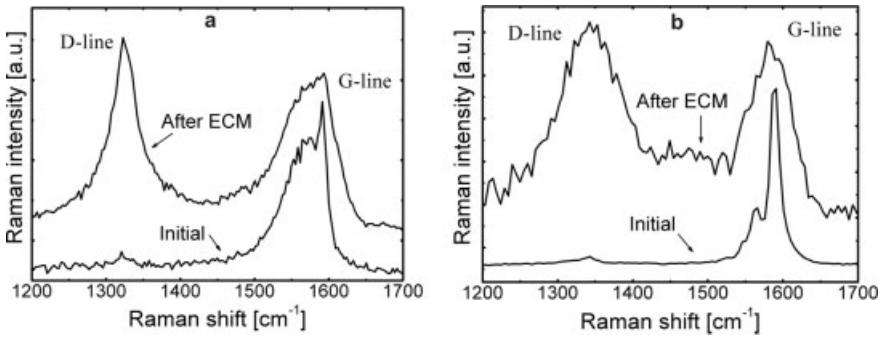

Fig. 4. a) Raman spectra of a metallic SWCNT before and after reductive ECM, acquired with the excitation wavelength of 647.1 nm. b) Raman spectra of a semiconducting SWCNT before and after reductive ECM, with an excitation wavelength of 514.5 nm. The D-line is found to be stronger than the G-line after the modification in both cases.

In order to obtain a more detailed overview of the effect of the two types of ECM on the various SWCNTs, a statistical analysis of the changes in the relative D-line intensities was carried out. For that purpose, we calculated the Raman intensity quotient by dividing the relative D-line intensities after and before ECM ($[I_D/I_G]^{after}/[I_D/I_G]^{before}$; where I_D and I_G are the intensities of the D-line and G-line respectively). For the sake of comparison, we have also analyzed the intensity quotients of several non-contacted nanotubes, which have been exposed to the same chemicals without applying a potential. The intensity quotients of these non-contacted SWCNTs had a mean value close to 1. For the metallic SWCNTs modified by oxidative amine (**A**) coupling, a narrow distribution around a mean value of ~1.5 was obtained. The reductive diazonium (**B**) coupling, in contrast, resulted in a broad distribution of intensity quotients, ranging between 1 and 20 centered around a mean value of ~8. Similar results were obtained on the semiconducting SWCNTs.

In view of the results presented above, we conclude that upon oxidative ECM with **A** the SWCNTs remain electronically unchanged, which suggests that no bonds are broken upon modification. Hence, we assume that the coating by the grafted films takes place via electropolymerization of the amine[20] without the formation of covalent bonds between the oxidatively created radicals and the nanotubes (Fig. 5a). In agreement with the preserved electrical properties, the unaffected Raman spectra of the modified metallic SWCNTs reveal that no structural deterioration of the nanotubes occurs under the oxidative grafting of the layers.

The increase in resistance upon oxidative ECM of semiconducting SWCNTs—which is not observed for the metallic nanotubes—can be explained by considering the fact that SWCNTs contacted by noble metal electrodes behave as p-type semiconductors[21] where the conductivity can be re-

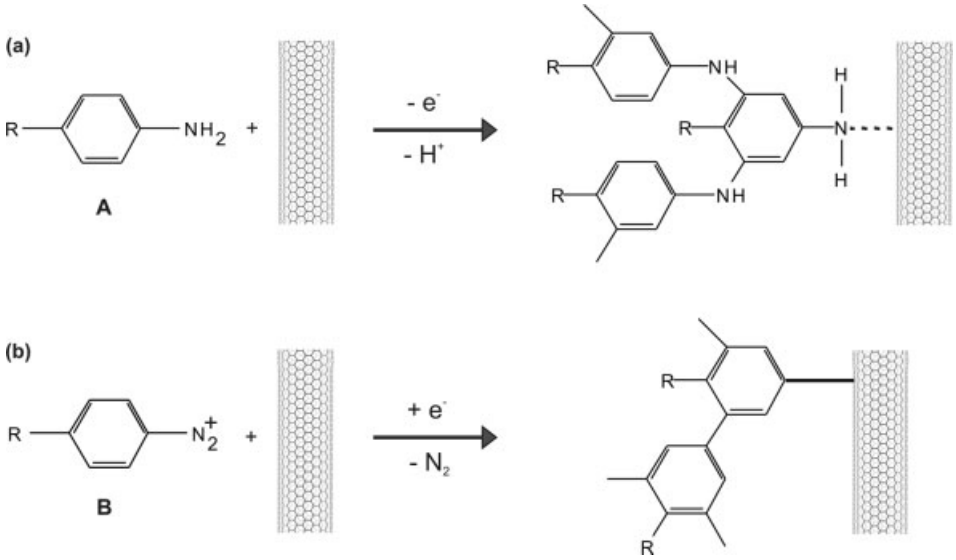

Fig. 5. Reaction schemes for a) oxidative ECM with **A** and b) reductive ECM with **B**. The broken line in part (a) indicates the formation of electropolymerized layers of **A** on the SWCNT without the creation of a chemical bond. In case of ECM with **B**, the experimental data give a strong indication of the formation of a chemical bond with the nanotube (bold line).

ADVANCED MATERIALS

duced by applying a positive gate voltage.[22] Since the polymeric layer formed on the SWCNTs contains amino-functions that are most likely protonated and therefore positively charged, these positive charges in close proximity to the nanotube surface are expected to reduce the hole concentration and thereby increase the nanotube resistance, similar to surface charge effects observed in sensors based on inorganic semiconductor nanowires.[23]

In the case of reductive ECM with **B**, the pronounced increase of both the electrical resistance and the intensity of the D-line indicates that the reductively created phenyl radicals form covalent (C–C) bonds to the nanotube (Fig. 5b), associated with the introduction of a sizeable density of sp^3-hybridized carbon atoms. The observed spread in the Raman intensity quotients may be explained by the fact that the reactivity of SWCNT side-walls decreases with increasing tube diameter.[9,24] Accordingly, the diazonium-modified tubes that showed only minor changes in the D-line could belong to the largest diameter tubes within the present sample ($d > 1.4$ nm).

In summary, we have employed electrical transport measurements and confocal Raman spectroscopy to study the properties of individual SWCNTs with electrochemically grafted molecular layers originating from two different coupling agents. The combination of both techniques allowed us to conclude that in the oxidative case, the SWCNTs are coated with a polymeric layer without the formation of covalent bonds. In the reductive case, on the contrary, there is a strong indication of the formation of chemical bonds with the atoms of the carbon nanotube. In future work, scanning tunneling spectroscopy and low temperature transport measurements may be applied in order to further deepen the understanding of the effect of the grafted molecular layers on the electronic and structural properties of the SWCNTs.

Experimental

Sample Preparation: SWCNTs with an average diameter of 1.3–1.4 nm, obtained from the arc discharge process (Carbolex, Lexington, KY), were dispersed in an aqueous surfactant solution (1 wt.-% lithium dodecyl sulfate) and purified by centrifugation. This suspension was placed on a highly doped silicon substrate (serving as back gate in the electrical measurements) with a thermally grown 100 nm SiO_2 layer, after the substrate surface had been treated for 2 min in an aqueous solution of *N*-(3-(trimethoxysilyl)propyl)-ethylenediamine. After an adsorption time of 30 min, the substrate was dried in a stream of nitrogen, and then rinsed with ultra-pure water and rinsed again. Electrodes were defined using a standard two-layer resist electron beam lithography procedure, and formed by evaporating a 15 nm layer of AuPd.

Electrochemical Modification: The electrochemical modification was carried out in a micro cell (capacity ~ 500 μL) with platinum counter and pseudoreference electrodes. A tungsten needle probe was used to make contact with the electrodes on the substrate surface, which enabled the functioning of the SWCNTs as the working electrode. A Solartron 1285 potentiostat was used for potential control. The oxidative coupling of 4-aminobenzylamine, $H_2N(C_6H_4)$-CH_2NH_2, (**A**; 10 mM) was performed in ethanol containing 0.1 M $LiClO_4$ as the supporting electrolyte by applying a potential of +0.75 V versus Pt. Reductive coupling of 4-nitrobenzene diazonium tetrafluoroborate, $O_2N(C_6H_4)$-$N_2^+BF_4^-$, (10 mM) was performed with 0.1 M $LiClO_4$ in *N*,*N*-dimethylformamide at a potential of (– 1.3 V) versus Pt. In both the coupling schemes, the potential was applied for a time of 120 s to obtain a thick coating that is easily detectable by AFM.

Characterization: The AFM images were acquired using a Digital Instruments Nanoscope IIIa apparatus in tapping mode using commercially available silicon cantilevers. The electrical transport measurements were carried out under ambient conditions with a Keithley sourcemeter 2400 and a Keithley multimeter 2000. Metallic SWCNTs were identified by almost no variation of the conductance when varying the gate voltage in the range of ± 10 V. Semiconducting SWCNTs show a change in conductance of 1 to 3 orders of magnitude under the same conditions. Confocal scanning images and Raman spectra were obtained at room temperature using an inverted Zeiss microscope equipped with a piezo scanner (Physical Instruments) and a high numerical aperture (NA) microscope objective (100x, NA = 0.9). Circularly polarized laser light (0.5 mW power) was focused down to a diffraction-limited spot size corresponding to an excitation power of 250 kW cm^{-2}. To obtain the images, this spot was raster-scanned over the substrate surface and the back reflected light was guided to an EG&G avalanche photo diode with optical filters or a monochromator being used to eliminate the scattered light. The images are of size 256 × 256 pixels obtained with an integration time of 15 ms/pixel. All spectra were recorded using a liquid nitrogen cooled charge coupled device (CCD) camera (Princeton) behind a 500 mm single grating spectrograph (Acton) with a highest resolution of 2 cm^{-1}.

Received: March 19, 2003
Final version: June 5, 2003

[1] R. Saito, G. Dresselhaus, M. S. Dresselhaus, *Physical Properties of Carbon Nanotubes*, Imperial College Press, London **1998**.
[2] M. A. Reed, *Molecular Electronics*, Academic Press, London **2000**.
[3] T. W. Odom, J. L. Huang, P. Kim, C. M. Lieber, *J. Phys. Chem. B* **2000**, *104*, 2794.
[4] J. M. Bonard, N. Weiss, H. Kind, T. Stöckli, L. Forro, K. Kern, A. Chatelain, *Adv. Mater.* **2001**, *13*, 184.
[5] M. Bockrath, D. H. Cobden, P. L. McEuen, N. G. Chopra, A. Zettl, A. Thess, R. E. Smalley, *Science* **1997**, *275*, 1922.
[6] S. J. Tans, R. M. Verschueren, C. Dekker, *Nature* **1998**, *393*, 49.
[7] J. Kong, N. R. Franklin, C. Zhou, M. G. Chapline, S. Peng, K. Cho, H. Dai, *Science* **2000**, *287*, 622.
[8] A. Bachtold, P. Hadley, T. Nakanishi, C. Dekker, *Science* **2001**, *294*, 1317.
[9] J. L. Bahr, J. M. Tour, *J. Mater. Chem.* **2002**, *12*, 1952.
[10] A. Hirsch, *Angew. Chem.* **2002**, *114*, 1933.
[11] V. Georgakilas, K. Kordatos, M. Prato, D. M. Guldi, M. Holzinger, A. Hirsch, *J. Am. Chem. Soc.* **2002**, *124*, 760.
[12] J. B. Cui, M. Burghard, K. Kern, *Nanolett.* **2002**, *2*, 117.
[13] J. B. Cui, R. Sordan, M. Burghard, K. Kern, *Appl. Phys. Lett.* **2002**, *81*, 3260.
[14] J. L. Bahr, J. Yang, D. V. Kosynkin, M. J. Bronikowski, R. E. Smalley, J. M. Tour, *J. Am. Chem. Soc.* **2001**, *123,* 6536.
[15] S. E. Kooi, U. Schlecht, M. Burghard, K. Kern, *Angew. Chem. Int. Ed.* **2002**, *41*, 1353.
[16] A. Mews, F. Koberling, T. Basché, G. Philipp, G. S. Duesberg, S. Roth, M. Burghard, *Adv. Mater.* **2000**, *12*, 1210.
[17] M. S. Dresselhaus, P. C. Eklund, *Adv. Phys.* **2000**, *49*, 705.
[18] J. Maultzsch, S. Reich, C. Thomsen, S. Webster, R. Czerw, D. L. Carrol, S. M. C. Vieira, P. R. Birkett, C. A. Rego, *Appl. Phys. Lett.* **2002**, *81*, 2647.
[19] J. Zhao, C. Jiang, Y. Fan, M. Burghard, T. Basché, A. Mews, *Nanolett.* **2002**, *2*, 823.
[20] A. J. Downard, *Electroanalysis* **2000**, *12*, 1085.
[21] R. Martel, T. Schmidt, H. R. Shea, T. Hertel, P. Avouris, *Appl. Phys. Lett.* **1998**, *73*, 2447.
[22] J. Nygard, D. H. Cobden, M. Bockrath, P. L. McEuen, P. E. Lindelof, *Appl. Phys. A* **1999**, *69*, 297.
[23] Y. Cui, Q. Wei, H. Park, C. M. Lieber, *Science* **2001**, *293*, 1289.
[24] Y. Chen, R. C. Haddon, S. Fang, A. M. Rao, P. C. Eklund, W. H. Lee, E. C. Dickey, E. A. Grulke, J. C. Pendergrass, A. Chavan, B. E. Haley, R. E. Smalley, *J. Mater. Res.* **1998**, *13,* 2423.

